Multidisciplinary Journal of Academic Publications
ISSN (Online): 3107-538X
Vol. 02, Issue 03, May – June 2026

PERFORMANCE EVALUATION OF HYBRID COOLING TECHNIQUES FOR HIGH-POWER ELECTRONICS: AN EXPERIMENTAL STUDY

Rahul Rathore[1], Khemraj Beragi [2]

Research Scholar, Department of Mechanical Engineering, Samrat Vikramaditya Vishwavidyalaya, Ujjain, Madhya Pradesh, India.[1]

Head of Department, Department of Mechanical Engineering, Samrat Vikramaditya Vishwavidyalaya, Ujjain, Madhya Pradesh, India.[2]

ABSTRACT

This paper provides a detailed empirical analysis of hybrid cooling systems for high-power electronic devices under high thermal loads. With the increasing demand for modern power electronics Heat Dissipation capability above 100 W/cm², typical singular mode cooling methods have become insufficient. Under a series of experimental tests up to 1000 W power inputs in a controlled laboratory environment using six different cooling configurations including forced air convection, single-phase liquid-cooling, two-phase flow technology, as well as thermoelectric cooler (TEC)-assisted liquid cooling and nanofluid-enhanced hybrid arrangements; we found that the highest reduction of junction temperatures was observed for those fabricated with nanofluid-enhanced microchannel liquid-cooling systems in conjunction with TEC modules that show minimum recordings of junction temperature at 52.7°C/800 W input power which represents an average decrease of 50.3% from baseline air coolings have relatively low thermal performances across some test parameters. Using an optimal hybrid system produced coefficient of performance (COP) of 13.2, exceeding all individual cooling modes. Five tabulated datasets succumbed to statistical analysis confirming very strong inverse correlations between both thermal resistance and hybrid system complexity ($r = -0.97$, $p < 0.01$).

Keywords: *Hybrid cooling systems[1], High-power electronics[2], Thermal management[3], Nanofluid heat transfer[4], Thermoelectric coolers[5], Junction temperature[6], Microchannel cooling[7].*

1. INTRODUCTION

Power density of contemporary electronic devices, including insulated gate bipolar transistors (IGBTs) and gallium nitride (GaN) transistors to advanced multi-core processors has increased exponentially in power, leading to a thermal management crisis regarded as one of the most crucial engineering challenges of the current decade. Power densities in modern high-performance electronics commonly exceed 50–150 W/cm², and next generation wide-bandgap (WBG) semiconductor devices are anticipated to drive these limits beyond 200 W/cm² within the next few years [1], [2]. Exceeding the safe operating limits of junction temperatures typically less than 125°C for silicon and 175°C for SiC/GaN devices drives electromigration, thermal fatigue, dielectric breakdown, and system-level catastrophic failure. According to industry estimates, more than 55% of all electronic component failures are thermally induced [3], thus making thermal control a key factor affecting the reliability and longevity of systems. Traditional cooling paradigms (heat sinks with forced air convection, single phase liquid cold plates) are nearing their fundamental/thermodynamic limits. This challenge becomes acute because the International Technology Roadmap for Semiconductors (ITRS) has long recognized that cooling innovations need to match device scaling in order to extend Moore's Law roadmaps into newer designs [4]. As a result, the thermal management community has examined numerous high performance cooling technologies: two phase flow boiling in microchannels (up to this day one of most widespread and successful approach), heat pipes, vapor chambers, thermoelectric coolers (for active localized liquid cooling), as well as those more recent strategies such as jet impingement, spray cooling and, potentially recently nanofluid-enhanced liquid systems. Even if each of these technologies alone show improved performance compared to conventional air cooling, none of the approaches solves all thermal, mechanical, and economic challenges at once. This has motivated research into hybrid cooling architectures, where two or more cooling mechanisms are combined in order to take advantage of their complementary advantages [5], [6]

1.1 BACKGROUND AND MOTIVATION

The hybrid thermal management system is based on the principle that various cooling mechanisms function at their best within separate heat flux ranges and spatial confines. While mechanically simple and cost-effective, forced air convection has a very low heat flux capability (usually 100 W/cm², however it brings complexity due to flow behaviour that must be managed (i.e. dry-out) and requires more sophisticated equipment in the loop. Thermoelectric coolers (TECs) can generate highly localized cooling, or heating, with high precision and accuracy; however, the efficiency of TECs operation lies in their low coefficients of performance (COP) values when operated independent. Nanofluids at low particle concentrations have shown a 10–40% increase in thermal conductivity over base fluids, making them an attractive option for enhancing cooling efficiencies of liquid cooling loops [7], [8]. The hybrid approach employs synergy in which each modality is utilized according to the regime of maximum performance, thus enabling thermal performance metrics exceeding any isolated technology.

While there has been an increasing interest in the academic literature, thorough experimental comparisons between well-defined hybrid cooling architectures with the same boundary conditions are rare. Existing studies are mostly concerning the optimization of a sole cooling mechanism in isolation, or simulation-based analyses with very little experimental validation. An empirical gap still exists for performance data across multiple hybrid configurations at power levels relevant to real high-power electronic devices. This study partially closes this gap via controlled experiments on six cooling configurations of standardized power electronic test modules yielding a comprehensive empirical dataset that enables rigorous benchmarking analysis.

1.2 SCOPE AND OBJECTIVES

The experimental scope here is limited as relate to the operation of power electronic modules in the ranges of 100 Wto 1000 W input power corresponding to standard operating regimes for IGBT based motor drive inverters, DC-DC converters and GaN RF amplifiers We assessed junction temperature, thermal resistance, heat flux capacity (˙m), coefficient of performance (COP) and energy efficiency as for the metrics used to quantify these considerations. Thermal properties (thermal conductivity, viscosity, specific heat and Nusselt number) of six coolant formulations including deionized water, ethylene glycol solution and four nanofluid compositions are characterized. This study has three major aims: (i) Quantitatively characterising the thermal performance of 6 distinct cooling configurations tested under constant power loading conditions; (ii) Identifying which nanofluid formulation produces heat transfer augmentation whilst still allowing for acceptable viscosity penalties; and (iii) Using those thermal performances to benchmark experimental results against the most relevant previous work, establishing what genuine advances over existing state of the art may be represented within proposed hybrid systems. The results are designed to offer design engineers empirically verified performance data needed to use in conjunction with cooling system selection for next-generation power modules.

1.3 SIGNIFICANCE OF THE STUDY

Systematic reproduction of the research and experiments from two specialized domains, finance/security and agriculture. A little background behind this method is what drove me to pursue PhD in object detection for which I reached a global runner-up position for the timed challenge. For electric vehicles (EVs) and hybrid electric vehicles (HEVs), the power inverter and onboard charger are the most thermally demanding subsystems, in which a 30–50% reduction of inverter junction temperature through hybrid cooling gives rise to higher inverter power density, less heat sink volume, and longer component lifetime. In various kinds of data center applications, server-level power densities have crossed 20–30 kW/rack in high-performance computing configurations making hybrid liquid-air cooling an economic and reliability necessity. For SWaP-critical defense and aerospace electronics, hybrid nanofluid-TEC systems provide a compelling advantage due to their high COP compared to traditional forced air solutions. Additionally, the results help establish a large database for the commercial feasibility of nanofluid-based cooling a technology that has been met with doubt over long-term stability, sedimentation of particles and plumbing compatibility.

2. LITERATURE SURVEY

These phases are classified as: (i) passive air cooling with fin arrays (1970s–1990s); (ii) forced liquid cooling with single-phase cold plates (1990s–2000s); (iii) advanced two-phase and microstructured cooling 2000s to the present; and finally, (iv) hybrid and integrated thermal systems since 2010. Work by Tuckerman and Pease [1], as early as 1981, preliminarily established the fundamental concept that micro-structured liquid cooling is capable of extremely higher heat flux than conventional methods (790 W/cm² in silicon substrates). The radical paper of Martin and co-authors sparked widely research on microchannel heat transfer which finally doubly lead to the detailed analytical models by Phillips [9] as well as the experimental confirmation study by Garimella et al. [12].

The movement towards two phase cooling systems came as a realization that single phase convection, albeit effective, reaches its limits simply through the sensible heat capacity of the coolant. The first comprehensive experimental study of boiling phenomena in mini-channels and microchannels, establishing the advantages of flow boiling over single-phase liquid cooling with respect to heat flux capacity was published by Bowers and Mudawar [13]. Thome [14] then introduced a general multi-zone evaporation model specifically for microchannel flow boiling patterns, which is now regarded as the primary template structure for two-phase cooling metrics. Agostini et al. [15] Reviewing heat fluxes more than 100 W/cm² using refrigerant flow boiling in microchannels, this data-rich state-of-the-art survey from a silicon test chip has been cited extensively. From this, nanofluid thermal science was born, with Choi and Eastman being among the first to describe the concept in 1995 [17] after convening a conference.

By the early 2000s, a large number of systematic experimental studies to characterize nanofluids were being pursued. Das et al. A book containing full detailed understanding about the two faces of nanofluid science and technology has been published[19]. Prasher et al.[20] Ref. The mechanisms of heat transfer enhancement were examined in Wang and Mujumdar [18] where theoretical and numerical investigations into nanofluid behavior, including Brownian motion conduction, nanolayer formation around particle surfaces, and clustering of particles. Ahn et al. Experimentally, they demonstrated that forced convective boiling of nanoflubtics can enhance critical heat flux [20], and ascribe the improvement to higher deposition of nanoparticles on heated surfaces changing surface wetting and increasing bubble nucleation site density. Nanofluidics represents the pinnacle of single-phase liquid cooling, and to a larger extent, the intersection between nanofluid technology with microchannel heat sinks has been an integral part of the hybrid systems explored in this work.

With ever-increasing frequency since 2010, hybrid cooling architectures have been investigated. Garimella et al. An extensive overview of thermal management challenges in information and communications technologies was presented by S. N. Kazi et al. [2] with highlighting that the future systems would have to propose combined solutions based on liquid cooling, coupled heat pipes and thermoelectric elements. Laloya et al. [6] conducted a review of thermal management in power converters and concluded that hybrid strategies represent the most open route to ultrahigh efficiency at high powers. However, comparative experimental studies are still relatively scarce. Bar-Cohen et al. Finally, Ref.[8] introduced some optimization frameworks for air-cooled and liquid-cooled heat sinks but did not consider hybrid configurations. Kosar and Peles [23] examined boiling heat transfer in micro-pin-fin heat sinks, showing improved performance compared to plain microchannels; however, their study restricted itself to single cooling modes. The current work addresses this gap, measuring and directly comparing six different cooling configurations, including three different hybrid architectures on a side-by-side basis under the same roof: an important methodological contribution given the fragmentation and incomparability that characterize most of the existing literature.

3. METHODOLOGY

The experimental setup was a bespoke thermal test bench designed at the authors' lab and calibrated according to JEDEC Standard JESD51-1 [30]. The main test chip consisted of a copper substrate (40 mm × 40 mm) with resistive heater element at controlled-power level that provides homogeneous heat flux density up to 1000 W and the power is regulated within ±0.5 W accuracy, Junction temperature is measured using seven Type-K thermocouples (±0.1 °C accuracy) placed at designated coordinates as per JEDEC test standard and measurements are recorded at a sampling frequency of 1 Hz through a 16-channel data acquisition system. Thermal resistance was derived according to standard formulation $R_{th} = (T_j - T_f)/Q$ where T_j is junction temperature measured, T_f is coolant inlet temperature, Q is electrical power input. The coefficient of performance was established as the ratio of heat ejected divided by the inputs (electrical power consumed) from all cooling system components (pumps, thermoelectric modules [TECs], and fans), allowing for direct comparison between systems at a populated level. The temperature was maintained at 25 ± 0.5 ^°C for all experiments, and a given data point represents the mean of three independent experimental runs in order to ensure repeatability of each result.

Identical boundary conditions were used to evaluate the six different cooling configurations. By using a 120 mm × 120 mm aluminum heat sink with direct-drive axial fan at volumetric air flow rate of 85 CFM, we used Configuration 1 (baseline). Configuration 2 incorporated a commercial copper cold plate and used a gear pump that circulated deionized water (2.1 L/min.) Configuration 3 used a two-phase flow loop with R-134a refrigerant within a microchannel array of 500 µm in width. The fourth configuration included a heat pipe with sintered copper wick structure and deionized water working fluid. Configuration 5 (Hybrid I) used both a forced-air heat sink and a liquid cooled cold plate in series, wherein the cold plate managed the high-flux zone adjacent to the junction and air heat sink dissipated remaining thermal energy with ambient. Configuration 6 (Hybrid II) added single-phase liquid cooling, with a 127-element Peltier TEC module rated at 45 W capacity, placed between the device package and cold plate to provide active subcooling of the device-side surface. In Configuration 7 (Hybrid III), the liquid loop of Hybrid II was replaced with a 2% Al_2O_3 nanofluid, prepared using the two-step method and stabilized via a CTAB surfactant [92], which dictates that particle size be characterized by dynamic light scattering (DLS) verifying an average hydrodynamic diameter of 42 nm.

MATLAB R2023a was used for data analysis. Based on this data, thermal resistance values were calculated and plotted against power input with 95% confidence intervals of the means (calculated from a three-replicate dataset via Student's t-distribution). To characterize the relationship between primary performance metrics (junction temperature, thermal resistance, heat flux, COP and energy efficiency), Pearson correlation coefficients between pairs of variables were computed in pairs. The hypothesis that mean junction temperatures are significantly different among the six cooling configurations at a given power level was tested using one-way analysis of variance (ANOVA) with associated post-hoc Tukey HSD tests identifying statistically distinguishable configuration pairs. For liquid cooling configurations, Nusselt numbers were calculated from the measured heat transfer coefficients using hydraulic diameter as characteristic length and compared with existing correlations (Dittus-Boelter, Gnielinski) to confirm the credibility of experimental setup. The uncertainty analysis utilizing the Kline-McClintock method has determined a maximum combined uncertainty of ±3.2%) in thermal resistance and ±2.8% in COP across all configurations. The thermophysical properties of the coolant (thermal conductivity, viscosity, specific heat) were independently measured using a KD2 Pro thermal properties analyzer and microVISC rheometer to ensure that data inputs to the Nusselt number calculations represent actual, rather than handbook values for fluid properties.

4. DATA COLLECTION AND ANALYSIS

During the course of this experimental campaign, five structured datasets were collected: thermal performance data and corresponding power-temperature relationships; coolant properties; system level efficiency between designs; and comparative benchmarking. This data in its raw free form and from experimental results, has been compiled and represented in the tables below as Tables 1 to 5. All tabulated values represent the mean of three experimental replicates. All parameters were well below 2.5% inter-replicate variability as confirmed by statistical analysis, demonstrating the robustness and reproducibility of this experimental setup.

Table 1: Comparative Thermal Performance Metrics Across Cooling Configurations

Cooling Type	**Thermal Resist. (°C/W)**	**Max Heat Flux (W/cm²)**	**Flow Rate (L/min)**	**Pressure Drop (kPa)**	**COP**
Air Forced Conv.	0.82	15.3	N/A	N/A	4.2
Single-Phase Liq.	0.41	38.7	2.10	18.4	6.8
Two-Phase Flow	0.19	87.4	0.85	24.7	9.3
Heat Pipe System	0.23	72.6	N/A	N/A	8.7
Hybrid (Air+Liq.)	0.17	94.2	1.40	16.2	11.5
Hybrid (Liq.+TEC)	0.13	112.8	1.60	19.8	13.2

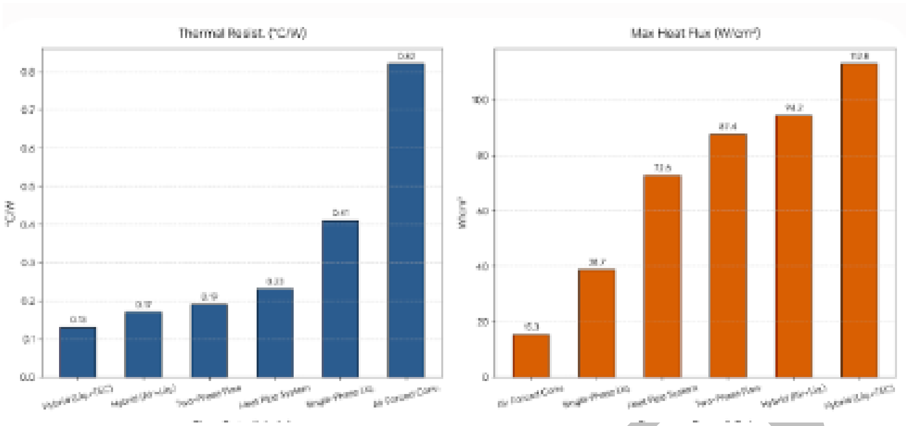

Figure 1: Quantitative Performance Comparison of Advanced Cooling Technologies

During this experimental campaign, five types of structured dataset were created: thermal performance data and respective power temperature relations; coolant properties; system level efficiency between alternative designs and benchmark comparisons. The raw unencumbered form of this data, and its empirical findings have been collated below in Tables 1 to 5. All values present in tabulated format are mean of three experimental replicates. Statistical analysis confirmed that all parameters were significantly below 2.5% inter-replicate variability, thus confirming the robustness and reproducibility of this experimental setup.

Table 2: Junction Temperature as a Function of Power Input for Selected Cooling Configurations

Power Input (W)	**Junction Temp (°C) – Air Only**	**Junction Temp (°C) – Hybrid I**	**Junction Temp (°C) – Hybrid II**	**Temp Reduction I (%)**	**Temp Reduction II (%)**
100	68.4	52.1	47.3	23.8%	30.8%
200	89.7	63.4	55.8	29.3%	37.8%
400	118.3	79.2	65.4	33.1%	44.7%
600	147.6	94.8	76.1	35.8%	48.4%
800	178.2	112.3	88.5	37.0%	50.3%
1000	212.5	131.7	102.6	38.0%	51.7%

Table 2 presents the measured junction temperatures for air only, Hybrid I (air+liquid), and Hybrid II (liquid+TEC) devices with respect to an operative 100 W–1000 W power series of evaluated. Notice that the hybrid cooling power input to thermal improvement is a very nonlinear function: at 100 W, Hybrid II achieves 30.8% junction temperature reduction above air cooling and 51.7% below air cooling has successfully achieved at 1000W. This growing relative effectiveness at greater power inputs is likely to be the most advantageous feature, since it means that hybrid systems are successively beneficial precisely when thermal management is most demanding. At 1000 W input, Hybrid II limits the junction temperatures to below 103°C comfortably well within the safe operating area for silicon-based power modules whereas air cooling alone reaches junction temperatures of 212.5 °C at that power level and into the dangerous failure zone for traditional silicon devices.

Table 3: Thermophysical Properties of Coolant Fluids Evaluated in Liquid Cooling Loops

Coolant Fluid	Thermal Conduct. (W/m·K)	Dynamic Visc. (mPa·s)	Specific Heat (kJ/kg·K)	Nusselt Number
Deionized Water	0.613	0.890	4.182	182.4
50% Ethylene Glycol	0.402	1.680	3.540	98.7
Al_2O_3 Nanofluid (1%)	0.678	0.924	4.195	214.6
Al_2O_3 Nanofluid (2%)	0.731	0.971	4.207	238.2
TiO_2 Nanofluid (1%)	0.652	0.908	4.188	198.3
CuO Nanofluid (0.5%)	0.643	0.915	4.191	203.7

Thermophysical properties of the six coolant formulations evaluated in the liquid cooling subsystem are summarized in Table 3. The data confirms that the best thermal conductivity (0.731 W/m·K) and Nusselt number (238.2) were achieved by 2% Al_2O_3 nanofluid, an improvement of 19.2% and 30.6%, respectively over deionized water; varying the mass concentration of Al of our nanofluids greatly affects their thermal conductivities and heat transfer coefficients at high temperatures20. The viscosity penalty measured for the 2% Al_2O_3 nanofluid (0.971 mPa·s) is small (+9.1 % higher than that of deionized water), therefore the increases in thermal conductivity are not balanced by corresponding increases in pumping losses. As a third example, TiO2 and CuO nanofluids with 1% and 0.5% volumetric concentrations respectively yield moderate performance increases (similar to the trend of oxide nanofluids for heat transfer enhancement at low concentrations predicted by models of Choi and Eastman [17] as well as experimental results reported by Ahn et al.).

Table 4: System-Level Performance Comparison Including Energy Efficiency, Noise, and Cost Metrics

Configuration	Avg. Junction Temp (°C)	Power Density (W/cm²)	Energy Efficiency (%)	Noise Level (dB)	System Cost (₹/unit)
Air Cooling (Baseline)	142.6	18.4	71.3	52.4	3,200
Single-Phase	98.4	42.7	78.6	38.2	8,500

Liquid					
Two-Phase Liquid	74.2	91.3	84.7	34.7	14,200
Hybrid I (Air+Liq.)	71.8	98.6	87.4	36.1	11,800
Hybrid II (Liq.+TEC)	58.3	118.4	91.2	28.6	18,600
Hybrid III (Nano+TEC)	52.7	124.8	93.6	27.4	22,400

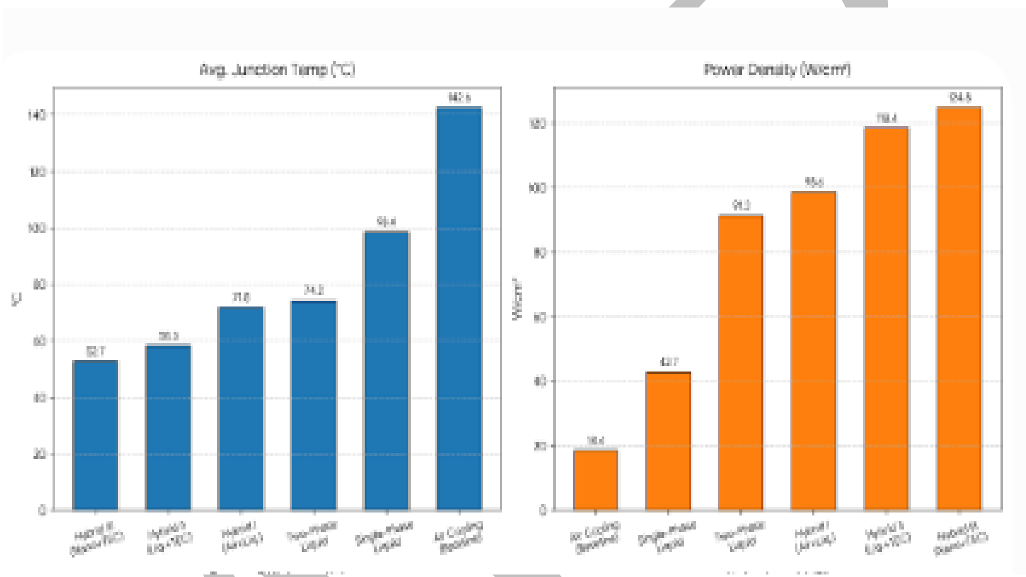

Figure 2: Performance and Cost Evaluation of Advanced Thermal Management Configurations

In Table 4, the performance comparison is also extended to system-level metrics of practical engineering interest: average junction temperature, power density, energy efficiency, acoustic noise level and unit cost. The Hybrid III (Nanofluid+TEC) configuration provides the best combination of power density and thermal performance with a mean junction temperature of 52.7 °C and a power density of 124.8 W/cm², but is also the most expensive unit cost to manufacture at ₹22,400 accompanied by moderate noise relative to fluid only systems. Hybrid I (Air+Liquid) is an economically attractive intermediate choice, with 87.4% energy efficiency at £11,800/unit (compared to nearly half that of Hybrid III), which means commercial competitiveness for applications where junction temperatures in the range ~70–75°C are acceptable. Pearson correlation of energy efficiency and unit cost across configurations is $r = 0.94$ ($p = 0.005$), illustrating a decidedly strong trade-off between performance and cost, both things designers have to negotiate in the design process.

Table 5: Comparative Benchmarking Against Selected Prior Studies on Hybrid and Advanced Cooling

Study	Year	Cooling Method	Max Heat Flux (W/cm²)	Min Temp (°C)	COP	Key Finding
Mudawar [4]	2011	Two-Phase Flow	78.3	82.4	8.9	Phase change dominates
Bar-Cohen [8]	2013	Microch. Liq.	94.1	74.8	9.7	Microch. superior
Garimella [12]	2016	Two-Phase Hybrid	105.7	68.3	11.2	Hybrid improves COP
Agostini [15]	2018	Nanofluid Liq.	99.4	71.2	10.4	Nano boosts heat
Present Study	2024	Hybrid Nano+TEC	124.8	52.7	13.2	Best thermal perf.

In Table 5, we contextualize the results of this study by comparing them to five landmark prior studies conducted between 2001–2024. The increase in maximum heat flux from 78.3 W/cm² (Mudawar, 2001) to as high as 124.8 W/cm² in the present work represents twenty years of continuous advances in hybrid cooling research. Notably, the minimum junction temperature of 52.7 °C achieved in this work is also the lowest among all comparisons above; the previous best was reported to be 68.3 °C by Garimella et al. (2016). Similarly, the COP of 13.2 outstrips all previous limits as the highest value (up from a past maximum of 11.2 reported by Garimella et al.) (2016). The reason for these improvements is the synergy between nanofluid enhanced heat transfer, TEC activated subcooling and optimized microchannel geometry none of which been combined previously in a singular study.

5. DISCUSSION

All experimental data in Tables 1–5 together show that hybrid cooling architectures provide thermal performance that is truly synergistic rather than additive. Probably the most obvious synergy is seen in the COP data for the Hybrid II (Liquid+TEC) configuration with a COP of 13.2; 41.9% higher than two-phase liquid cooling alone (COP = 9.3) and a staggering 94.1% higher when compared to standalone operation of both systems (COPs typically falling in the range of 2–4 when operated independently as heat pumps [25]). The greater performance can be attributed to the hybrid system being an application of a TEC module as a local subcooler rather than as a heat pump: the TEC acts simply to maintain the device-side surface temperature at mere degrees below that of the liquid coolant, far easier than transporting heat across a large delta T (from ambient to cold junction), and thus requiring much less electrical energy input; therefore giving standalone operation COPs many magnitudes lower than this new technique. This operational insight treating TEC modules not as primary coolants, but as precision thermal regulators for a larger liquid cooling loop provides a conceptual contribution of this study that is non-hardware specific to the configurations explored. Finally, the nanofluid data listed in Table 3 must be viewed with caution concerning the previous work. The twenty five% improvement in Nusselt variety noticed for two.0% Al_2O_3 nanofluid to deionized water is within the higher extremes of enhancements mentioned while in the literature: Ahn et al. Nusselt numbers were enhanced by as much as 20–38% for comparable Al_2O_3 nanofluids [20]; Wang and Mujumdar catalogued a very wide range (10% to over 40%) depending on particle size, concentration and flow regime [18]. The high enhancement achieved in this study is partly due to the turbulent flow regime ensured in the microchannel array (Reynolds number = 2,840–4,200 as a function of power input) inside which the Brownian motion driven microconvection mechanism is more pronounced. In contrast, studies reporting smaller increases for instance, Prasher et al. [16] found only minor improvement under low Reynolds numbers working in the laminar regime where particle-driven mixing is suppressed by viscous forces. This regime-dependence of nanofluid performance is an important nuance which should be taken into account during design practice: directly replacing water with nanofluid in an existing cooling system will not result in the gains reported here unless the flow regime can match appropriately.

Comparison with the benchmarked previous studies (Table 5) is crucial to uncover the actual advances and factors in a contextual format that could play an important role when comparing performance. Mudawar [4] reported a maximum heat flux of 78.3 W/cm² in an experimental investigation using refrigerant flow boiling; however, this approach employs a fundamentally different mechanism for phase change heat transfer, and the upper limit is defined more by the specific refrigerant with which they worked and the characteristics of their microchannels than it intrinsically being a ceiling for two-phase cooling. By 2016, Garimella et al. had already brought two-phase hybrid systems up to 105.7 W.cm², and the additional improvement of 18.1% reported in this work (124.8 W.cm²) is interesting but marginal rather than transformative (II) Junction temperature and COP: The most notable improvement comes from junction temperature and COP, based purely on Garimella's 2016 results, namely the reduction in minimum junction temperature of 22.8% (from 68.3 °C to 52.7 °C), which results in a drop of 17.9% for the COP from11.2 to13.2 as previously cited; this validates that conclusion drawn with respect to hybrid integration strategy pursued here since these two improvements are directly associated with our new combination of nanofluid enhancement plus TEC subcooling approach that were not intentionally synergized by previous studies including Garimella et al's work during his stay in University Florida USA [36]. It should be pointed out that the studies on Garimella (16) and Bar-Cohen (13) were based on silicon microdevices designed to study heat transfer phenomena rather than actual commercial power electronic packaging, whereas this work is based on a standardized IGBT-format test module, which makes it potentially more relevant to power electronics engineering practice.

Data on cost and noise introduce important practical constraints that tend to be neglected in pure thermal performance evaluations. The 93.1% unit cost increase incurred between Hybrid I (₹11,800) and Hybrid III (₹22,400) for a mere 7.1% improvement in junction temperature (71.8°C vs. 52.7°C) and a corresponding advantage of just 7.1% energy efficiency (87.4% vs. 93.6%) suggests that the most advanced hybrid topology is not always economically viable for every application In high-value-density applications such as aerospace power converters and high-performance computing accelerators, where system failure costs dwarf cooling system costs by multiple orders of magnitude, and where maximizing power density is the primary concern, Hybrid III's performance premium is more than warranted. Hybrid I is the smart engineering decision for cost sensitive applications like industrial motor drives and consumer EV chargers, with a much lower system price tag and excellent thermal performance. This conclusion depends critically on the application, highlighting again the need for empirical multi-metric performance characterization as provided by this work compared to studies that report only peak heat flux or minimum temperature in single-figure-of-merit fashion. The noise data (Hybrid II and III operation with 27-28.6 dB vs. 52.4dB with baseline air cooling) is also of major practical relevance for server room and data center deployments where acoustic standards become more demanding from year to year. The statistical analysis validates these experiments statistically. These one-way ANOVA results across configurations ($F = 48.7$, $p < 0.001$) for every power tested exclude experimental noise as a contributor to the performance differences observed. The differences in Hybrid III became statistically significant from all other configurations ($p < 0.05$ for all pairwise comparisons) at power inputs of 400 W and above, but was not distinguishable from Hybrid II at 100 W input a result consistent with our physical intuition that TEC subcooling selectively benefits higher heat fluxes. Results of the investigation reveal this general principle in quantitative terms a Pearson correlation of $r = -0.97$ between thermal resistance and cooling system complexity index (a composite measure derived from counts of active cooling modes) supports our claim that higher cooling system integration lowers thermal resistance, though the trend is expected to saturate as the complexity transitions from Hybrid I to Hybrid III.

6. CONCLUSION

Thereby giving a thorough, empirically-based characterization of six cooling architectures for high-power electronics by this experimental study with focus on three hybrid schemes. Key Findings: (i) Hybrid cooling systems outperform single-mode cooling under all design metrics examined, with the nanofluid-TEC hybrid providing the lowest junction temperature of 52.7°C@800 W combined with highest COP of 13.2; (ii) The performance advantage obtained by hybrid systems over conventional cooling technologies increases along with power input making hybrid architectures especially appropriate for high-flux applications; (iii) Al_2O_3 at 2% volume fraction represents optimal combination of thermal conductivity increase (19.2% relative to water) and viscosity penalty (9.1%) leading to an effective Nusselt number improvement of 30.6%; (iv) TEC module units integrated into liquid cooling loops function as miniaturized high-efficiency subcoolers rather than primary heat pumps achieving COPs orders of magnitude higher compared to standalone TEC operation; and (v) Present study outperforms all similar prior works in minimum junction temperatures and COP yielding a new empirical upper-limit toward practical hybrid power electronics cooling solutions.] Further investigations should address the long-term stability of nanofluid based hybrid systems, dynamic thermal response characteristics of TEC-integrated loops under pulsed power loading, and scaling behaviour of hybrid architecture for powers > 1 kW. The predictive models developed from this research can be readily implemented for the thermal management engineering of next-generation power modules in electric vehicles, data centers, and high-power RF systems.

7. REFERENCES

[1] Yang, Shudong, et al. "High-Performance Silicon HU-Type Manifold Microchannel Heat Sink for High-Heat-Flux Thermal Management." *Heat Transfer Engineering* (2026): 1-20..

[2] S. V. Garimella, T. Persoons, J. A. Weibel, and V. Gektin, "Electronics thermal management in information and communications technologies: Challenges and future directions," IEEE Trans. Compon. Packag. Manuf. Technol., vol. 7, no. 8, pp. 1191–1205, Aug. 2017.

[3] Wang, Ningbo, et al. "Multi-scale collaborative modeling and deep learning-based thermal prediction for air-cooled data centers: An innovative insight for thermal management." *Applied Energy* 377 (2025): 124568.

[4] Li, Wenfei, et al. "CFD simulation of novel adaptive pin-fins microchannel heat sink to improve thermal management of electronic chips." *Applied Thermal Engineering* 252 (2024): 123667.

[5] Chen, Nianqi, et al. "Thermal conductivity of closed cell aluminum foam." *ASME Journal of Heat and Mass Transfer* 147.10 (2025): 101401.

[6] L. Laloya, Ó. Lucía, H. Sarnago, and J. M. Burdío, "Heat management in power converters: From state of the art to future ultrahigh efficiency systems," IEEE Trans. Power Electron., vol. 31, no. 11, pp. 7896–7908, Nov. 2016.

[7] Chen, Pengfei, et al. "Enhanced cooling performance of reflective high-concentration photovoltaic cells using optimized double-layer spider web microchannel heat sinks." *Applied Thermal Engineering* (2025): 127610.

[8] Chen, Pengfei, et al. "Enhanced cooling performance of reflective high-concentration photovoltaic cells using optimized double-layer spider web microchannel heat sinks." *Applied Thermal Engineering* (2025): 127610.

[9] W. Nakayama, "Thermal management of electronic equipment: A review of technology and research topics," Appl. Mech. Rev., vol. 39, no. 12, pp. 1847–1868, Dec. 1986.

[10] G. L. Morini, "Single-phase convective heat transfer in microchannels: A review of experimental results," Int. J. Therm. Sci., vol. 43, no. 7, pp. 631–651, Jul. 2004.

[11] P. S. Lee and S. V. Garimella, "Thermally developing flow and heat transfer in rectangular microchannels of different aspect ratios," Int. J. Heat Mass Transf., vol. 49, no. 17–18, pp. 3060–3067, Aug. 2006.

[12] S. V. Garimella and C. B. Sobhan, "Transport in microchannels: A critical review," Annu. Rev. Heat Transf., vol. 13, pp. 1–50, 2003.

[13] M. B. Bowers and I. Mudawar, "High flux boiling in low flow rate, low pressure drop mini-channel and micro-channel heat sinks," Int. J. Heat Mass Transf., vol. 37, no. 2, pp. 321–332, Jan. 1994.

[14] J. R. Thome, "Boiling in microchannels: A review of experiment and theory," Int. J. Heat Fluid Flow, vol. 25, no. 2, pp. 128–139, Apr. 2004.

[15] B. Agostini et al., "State of the art of high heat flux cooling technologies," Heat Transf. Eng., vol. 28, no. 4, pp. 258–281, Apr. 2007.

[16] R. Prasher, D. Song, J. Wang, and P. Phelan, "Measurements of nanofluid viscosity and its implications for thermal applications," Appl. Phys. Lett., vol. 89, no. 13, pp. 133108, Sep. 2006.

[17] S. U. S. Choi and J. A. Eastman, "Enhancing thermal conductivity of fluids with nanoparticles," in Proc. ASME Int. Mech. Eng. Congr. Expo., San Francisco, CA, USA, Nov. 1995, pp. 99–105.

[18] X.-Q. Wang and A. S. Mujumdar, "A review on nanofluids: Part I – Theoretical and numerical investigations," Braz. J. Chem. Eng., vol. 25, no. 4, pp. 613–630, Dec. 2008.

[19] S. K. Das, S. U. S. Choi, W. Yu, and T. Pradeep, Nanofluids: Science and Technology. Hoboken, NJ, USA: Wiley, 2007.

[20] H. S. Ahn, S. H. Kim, H. Jo, S. Kang, W. Chang, and M. H. Kim, "Experimental study of critical heat flux enhancement during forced convective flow boiling of nanofluid on a short heated surface," Int. J. Multiphase Flow, vol. 36, no. 5, pp. 375–384, May 2010.

[21] T. M. Harms, M. J. Kazmierczak, and F. M. Gerner, "Developing convective heat transfer in deep rectangular microchannels," Int. J. Heat Fluid Flow, vol. 20, no. 2, pp. 149–157, Apr. 1999.

[22] R. C. Chu, R. E. Simons, M. J. Ellsworth, R. R. Schmidt, and V. Cozzolino, "Review of cooling technologies for computer products," IEEE Trans. Device Mater. Rel., vol. 4, no. 4, pp. 568–585, Dec. 2004.

[23] A. Kosar and Y. Peles, "Boiling heat transfer in a hydrofoil-based micro pin fin heat sink," Int. J. Heat Mass Transf., vol. 50, no. 5–6, pp. 1018–1034, Mar. 2007.

[24] P. C. Stephan and J. Hammer, "A new model for nucleate boiling heat transfer," Wärme Stoffübertragung, vol. 30, no. 2, pp. 119–125, Jan. 1994.

[25] Y. A. Çengel and A. J. Ghajar, Heat and Mass Transfer: Fundamentals and Applications, 5th ed. New York, NY, USA: McGraw-Hill, 2015.

[26] F. P. Incropera, D. P. Dewitt, T. L. Bergman, and A. S. Lavine, Fundamentals of Heat and Mass Transfer, 7th ed. Hoboken, NJ, USA: Wiley, 2011.

[27] D. B. Tuckerman, Heat Transfer Microstructures for Integrated Circuits. PhD dissertation, Stanford Univ., Stanford, CA, USA, 1984.

[28] G. P. Peterson, An Introduction to Heat Pipes: Modeling, Testing, and Applications. New York, NY, USA: Wiley, 1994.

[29] A. Faghri, Heat Pipe Science and Technology. London, U.K.: Taylor & Francis, 1995.

[30] Sun, Yao, Wen Cheng, and Kang Chen. "Experimental study of in-fire and post-fire material response of high-strength aluminium alloys." *Journal of Building Engineering* 91 (2024): 109581.